THE JOURNAL OF BIOLOGICAL CHEMISTRY VOL. 287, NO. 29, pp. 24064–24076, July 13, 2012

Myosin Regulatory Light Chain Diphosphorylation Slows Relaxation of Arterial Smooth Muscle*[S]

Received for publication, April 11, 2012, and in revised form, May 17, 2012 Published, JBC Papers in Press, May 31, 2012, DOI 10.1074/jbc.M112.371609

Cindy Sutherland and Michael P. Walsh[1]

From the Department of Biochemistry and Molecular Biology, Faculty of Medicine, University of Calgary, Calgary, Alberta T2N 4N1, Canada

Background: The regulatory light chains of smooth muscle myosin are phosphorylated at Ser^{19} and Thr^{18}.
Results: Phosphorylation at Thr^{18} does not increase force elicited by Ser^{19} phosphorylation, but reduces the rate of relaxation.
Conclusion: Diphosphorylation slows relaxation compared with monophosphorylation at Ser^{19}.
Significance: Knowledge of the functional effects of myosin diphosphorylation is important for understanding the underlying causes of hypercontractility.

The principal signal to activate smooth muscle contraction is phosphorylation of the regulatory light chains of myosin (LC_{20}) at Ser^{19} by Ca^{2+}/calmodulin-dependent myosin light chain kinase. Inhibition of myosin light chain phosphatase leads to Ca^{2+}-independent phosphorylation at both Ser^{19} and Thr^{18} by integrin-linked kinase and/or zipper-interacting protein kinase. The functional effects of phosphorylation at Thr^{18} on steady-state isometric force and relaxation rate were investigated in Triton-skinned rat caudal arterial smooth muscle strips. Sequential phosphorylation at Ser^{19} and Thr^{18} was achieved by treatment with adenosine 5′-*O*-(3-thiotriphosphate) in the presence of Ca^{2+}, which induced stoichiometric thiophosphorylation at Ser^{19}, followed by microcystin (phosphatase inhibitor) in the absence of Ca^{2+}, which induced phosphorylation at Thr^{18}. Phosphorylation at Thr^{18} had no effect on steady-state force induced by Ser^{19} thiophosphorylation. However, phosphorylation of Ser^{19} or both Ser^{19} and Thr^{18} to comparable stoichiometries (0.5 mol of P_i/mol of LC_{20}) and similar levels of isometric force revealed differences in the rates of dephosphorylation and relaxation following removal of the stimulus: $t_{1/2}$ values for dephosphorylation were 83.3 and 560 s, and for relaxation were 560 and 1293 s, for monophosphorylated (Ser^{19}) and diphosphorylated LC_{20}, respectively. We conclude that phosphorylation at Thr^{18} decreases the rates of LC_{20} dephosphorylation and smooth muscle relaxation compared with LC_{20} phosphorylated exclusively at Ser^{19}. These effects of LC_{20} diphosphorylation, combined with increased Ser^{19} phosphorylation (Ca^{2+}-independent), may underlie the hypercontractility that is observed in response to certain physiological contractile stimuli, and under pathological conditions such as cerebral and coronary arterial vasospasm, intimal hyperplasia, and hypertension.

Smooth muscle contraction is activated by an increase in cytosolic free Ca^{2+} concentration ($[Ca^{2+}]_i$), whereupon Ca^{2+} saturates the four Ca^{2+}-binding sites of calmodulin (1). $(Ca^{2+})_4$-calmodulin activates myosin light chain kinase (MLCK),[2] which catalyzes phosphorylation of the motor protein myosin II at Ser^{19} of its two 20-kDa regulatory light chain subunits (LC_{20}) (2). This simple phosphorylation reaction markedly increases the actin-activated MgATPase activity of myosin, which provides the energy for cross-bridge cycling and the development of force or shortening of the muscle (3). MLCK is also capable of phosphorylating LC_{20} at Thr^{18} *in vitro*, but this requires very high (unphysiological) concentrations of the kinase (4, 5). Relaxation follows the removal of Ca^{2+} from the cytosol, which inactivates MLCK, and myosin is dephosphorylated by myosin light chain phosphatase (MLCP), a type 1 Ser/Thr phosphatase (6).

We and others have demonstrated that smooth muscle contraction can be elicited in the absence of Ca^{2+} by treatment with inhibitors of type 1 protein phosphatases (7–19). For example, treatment of Triton-skinned rat caudal arterial smooth muscle strips with the membrane-impermeant phosphatase inhibitor microcystin in the absence of Ca^{2+} (presence of EGTA) elicited a slow, sustained contractile response that correlated with LC_{20} phosphorylation (16). Further investigation revealed that this Ca^{2+}-independent phosphorylation occurred at both Ser^{19} and Thr^{18}, referred to as diphosphorylation (16). The kinase responsible was shown not to be MLCK on the basis of the following observations: (i) purified MLCK is inactive in the absence of Ca^{2+} (20–22); (ii) LC_{20} diphosphorylation requires unphysiologically high MLCK concentrations (5); (iii) MLCK inhibitors have no effect on Ca^{2+}-independent, microcystin-induced LC_{20} diphosphorylation and contraction of Triton-skinned tissue (16, 19); (iv) removal of endogenous calmodulin by treatment of Triton-skinned smooth muscle strips with the calmodulin antagonist trifluoperazine in the presence of Ca^{2+} does not affect Ca^{2+}-independent, microcystin-induced LC_{20} diphosphorylation and contraction (23); (v)

* This work was supported in part by Canadian Institutes of Health Research Grant MOP-111262 (to M. P. W.).
[S] This article contains supplemental Figs. S1–S5 and Table S1.
[1] An Alberta Innovates-Health Solutions Scientist and Canada Research Chair (Tier 1) in Vascular Smooth Muscle Research. To whom correspondence should be addressed: 3330 Hospital Drive N.W., Calgary, Alberta T2N 4N1, Canada. Tel.: 403-220-3021; Fax: 403-270-2211; E-mail: walsh@ucalgary.ca.

[2] The abbreviations used are: MLCK, myosin light chain kinase; ATPγS, adenosine 5′-*O*-(3-thiotriphosphate); CaM, calmodulin; ILK, integrin-linked kinase; LC_{20}, the 20-kDa regulatory light chains of smooth muscle myosin II; MLCP, myosin light chain phosphatase; MYPT1, myosin targeting subunit of MLCP; ZIPK, zipper-interacting protein kinase; TES, 2-{[2-hydroxy-1,1-bis(hydroxymethyl)ethyl]amino}ethanesulfonic acid.

endogenous LC_{20} in smooth muscle myofilaments is phosphorylated in the absence of Ca^{2+} at Ser^{19} or Thr^{18} alone, as well as at both sites (16), whereas purified MLCK (at high concentration) only phosphorylates Thr^{18} after Ser^{19} has been phosphorylated (4); (vi) stimuli that induce maximal activation of MLCK in smooth muscle tissues (*e.g.* membrane depolarization of intact vascular smooth muscle strips with an optimal KCl concentration, or addition of a maximal concentration of Ca^{2+} to permeabilized strips) induce LC_{20} phosphorylation exclusively at Ser^{19} (23, 24); (vii) Ca^{2+}-independent LC_{20} kinase activity can be separated from MLCK chromatographically (16); and (viii) the Ca^{2+}-independent LC_{20} kinase, unlike MLCK, does not use ATPγS as a substrate (this study). We purified this Ca^{2+}-independent LC_{20} kinase activity from chicken gizzard myofilaments and identified it as integrin-linked kinase (ILK) (17). Bacterially expressed ILK phosphorylated LC_{20} in intact myosin in a Ca^{2+}-independent manner (17). Approximately 50% of cellular ILK was retained in Triton-skinned smooth muscle and may be associated with MLCP because purified phosphatase preparations contain co-purifying ILK (19). It should be noted that ILK has often been described as a pseudokinase (25), but the evidence for its bona fide kinase activity is substantial (26, 27). Zipper-interacting protein kinase (ZIPK) has also been implicated in the diphosphorylation of LC_{20} (18, 28), although inhibition of ZIPK activity in Triton-skinned rat caudal arterial smooth muscle did not affect microcystin-induced LC_{20} diphosphorylation or contraction (19), suggesting that ILK is likely the responsible kinase in these conditions.

The diphosphorylation site in LC_{20} is highly evolutionarily conserved: the sequence around Thr^{18}–Ser^{19} (Arg-Ala-Thr-Ser-Asn-Val-Phe-Ala-Met-Phe; residues 16–25), is identical throughout the animal kingdom and is also found in a homolog of LC_{20} (29) in the genome of the unicellular choanoflagellate *Monosiga brevicollis* (30); choanoflagellates appear to be the closest living relatives of metazoans (30, 31). LC_{20} isoforms are also found in non-muscle myosin II, and contain phosphorylation sites corresponding to Thr^{18} and Ser^{19} of smooth muscle LC_{20} that play an important role in regulation of motility (32).

The functional effects of phosphorylation of LC_{20} at Ser^{19} and Thr^{18} have been investigated *in vitro* using purified LC_{20} or intact myosin as substrates at high concentrations of MLCK. Ikebe and Hartshorne (4) showed that the actin-activated MgATPase activity of diphosphorylated myosin was 2–3-fold greater than that of myosin phosphorylated exclusively at Ser^{19}. This increase in actomyosin MgATPase activity can be attributed to a doubling of the V_{max} when both sites are phosphorylated (33–35). In the *in vitro* motility assay, however, myosin phosphorylated at both Ser^{19} and Thr^{18} moved actin filaments at a rate similar to myosin phosphorylated at Ser^{19} alone (35, 36).

LC_{20} diphosphorylation has been observed in various smooth muscle tissues treated with a variety of contractile stimuli (37–41), and several instances of diphosphorylation of LC_{20} have been reported in pathological conditions associated with hypercontractility (42–46). This prompted us to further investigate the functional effects of LC_{20} diphosphorylation in vascular smooth muscle.

EXPERIMENTAL PROCEDURES

Materials—All chemicals were analytical grade unless otherwise indicated and purchased from EMD Chemicals (Gibbstown, NJ). Triton X-100 and ATPγS were purchased from Sigma, microcystin-LR from Alexis Biochemicals (San Diego, CA), calyculin-A and okadaic acid from Calbiochem, and dithiothreitol (DTT) from ICN Biochemicals (Aurora, OH). Calmodulin (47) and MLCK (48) were purified from chicken gizzard as previously described. Antibodies to LC_{20} (polyclonal anti-pan LC_{20}) were from Santa Cruz Biotechnology (Santa Cruz, CA) and used at 1:500 dilution; phosphospecific antibodies to LC_{20} phosphorylated at Ser^{19} (monoclonal anti-pS19-LC_{20}) were from Cell Signaling (Danvers, MA) and used at 1:1,000 dilution; phosphospecific antibodies to LC_{20} phosphorylated at Thr^{18} (polyclonal anti-pT18-LC_{20}) were from 21st Century Biochemicals (Marlboro, MA) and used at 1:2,000 dilution; phosphospecific antibodies to LC_{20} phosphorylated at both Thr^{18} and Ser^{19} (polyclonal anti-pT18,pS19-LC_{20}) were from Cell Signaling and used at 1:500 dilution. Polyclonal phosphospecific antibodies to MYPT1 phosphorylated at Thr^{697} or Thr^{855} were purchased from Upstate USA (Charlottesville, VA) and used at 1:1,000 dilution. Polyclonal anti-actin was from Cytoskeleton Inc. (Denver, CO) and used at 1:1,000 dilution. Secondary antibodies coupled to horseradish peroxidase were purchased from Chemicon (Temecula, CA).

Buffer Compositions—HEPES-Tyrode (H-T) buffer contained 137 mM NaCl, 2.7 mM KCl, 1 mM $MgCl_2$, 1.8 mM $CaCl_2$, 5.6 mM glucose, 10 mM HEPES, pH 7.4. Ca^{2+}-free H-T buffer contained 140.6 mM NaCl, 2.7 mM KCl, 1 mM $MgCl_2$, 5.6 mM glucose, 10 mM HEPES, pH 7.4. Buffer A contained 30 mM TES, 0.5 mM DTT, 50 mM KCl, 5 mM K_2EGTA, 150 mM sucrose, pH 7.4. *p*Ca 9 solution contained 4 mM K_2EGTA, 5.83 mM $MgCl_2$, 0.5 mM dithioerythritol, 20 mM TES, pH 6.9, and an ATP regenerating system composed of 3.9 mM Na_2ATP, 7.56 mM potassium propionate, 16.2 mM phosphocreatine, and 30 units/ml of creatine kinase. The free [Ca^{2+}] of this *p*Ca 9 solution was determined to be 6 nM using fura-2. *p*Ca 4.5 solution contained 4 mM CaEGTA, 5.66 mM $MgCl_2$, 0.5 mM dithioerythritol, 20 mM TES, pH 6.9, and the ATP regenerating system.

Tissue Preparation and Force Measurements—Caudal arteries were removed from male Sprague-Dawley rats (300–350 g) that had been anesthetized with halothane and euthanized according to protocols consistent with the standards of the Canadian Council on Animal Care and approved by the University of Calgary Animal Care and Use Committee. The arteries were cleaned of excess adventitia and adipose tissue in Ca^{2+}-free H-T buffer. Segments were placed over a 0.31-mm needle and moved back and forth 40 times to remove the endothelium, cut into helical strips (1.5 × 6 mm), mounted on a Grass isometric force transducer (model FT03C) connected to a PowerLab (ADInstruments) 8-channel recording device with a resting tension of 0.45 g and incubated for 20 min in H-T buffer (bath volume = 0.8 ml). Tissues were stimulated at least twice with H-T buffer containing 87 mM KCl (the increase in [KCl] was balanced by a decrease in [NaCl]) with a 20-min interval of relaxation in Ca^{2+}-free H-T buffer. Muscle strips were then incubated in Ca^{2+}-free H-T buffer and either used

for experiments with intact tissue or were skinned (demembranated) as follows. Tissues for skinning were incubated for 5 min in Buffer A and subsequently demembranated by incubation for 2 h in Buffer A containing 1% (v/v) Triton X-100. Skinned tissues were then washed 3 times (5 min each) in *p*Ca 9 solution prior to treatments described in the figure legends.

Quantification of LC_{20} Phosphorylation Levels—At selected times during experimental protocols, tissues were immersed in cold 10% trichloroacetic acid, acetone, 10 mM DTT, washed three times (1 min each) with acetone/DTT, and lyophilized for 36 h. Dried tissues were immersed in 1 ml of SDS gel sample buffer (2% (w/v) SDS, 100 mM DTT, 10% (v/v) glycerol, 0.01% bromphenol blue, 60 mM Tris-HCl, pH 6.8), heated to 95 °C for 2 min, cooled to room temperature, and rotated overnight at 4 °C. Samples (40 μl) were subjected to phosphate affinity SDS-PAGE using an acrylamide-pendant phosphate-binding tag (Phos-tag SDS-PAGE with 12.5% acrylamide) at 30 mA/gel for 70 min in mini-gels in which 0.05 mM Phos-tag acrylamide (NARD Institute, Japan) and 0.1 mM $MnCl_2$ were incorporated into the running gel (49). Separated proteins were transferred to PVDF membranes (Roche Applied Science) overnight at 27 volts and 4 °C in 25 mM Tris-HCl, pH 7.5, 192 mM glycine, 10% (v/v) methanol. Proteins were fixed on the membrane by treatment with 0.5% glutaraldehyde in phosphate-buffered saline (137 mM NaCl, 2.68 mM KCl, 10 mM Na_2HPO_4, 1.76 mM KH_2PO_4) for 45 min. Membranes were then incubated with 5% nonfat dried milk in Tris-buffered saline containing Tween (TBST: 20 mM Tris-HCl, pH 7.5, 137 mM NaCl, 3 mM KCl, 0.05% Tween 20) for 1–2 h, followed by primary antibody in TBST overnight at 4 °C. Following washout of the primary antibody, membranes were incubated with secondary antibody (anti-rabbit or anti-mouse IgG-horseradish peroxidase conjugate in TBST at 1:10,000 dilution) for 2 h at room temperature, washed with TBST (4 × 5 min), and then with TBS (1 × 5 min) before chemiluminescence signal detection using the Super-Signal West Femto reagent (Thermo Scientific, Rockford, IL). The emitted light was detected and quantified with a chemiluminescence imaging analyzer (LAS3000mini; Fujifilm) and images were analyzed with MultiGauge version 3.0 software.

Data Analysis—Values are presented as the mean ± S.E., with *n* indicating the number of animals used; several muscle strips were used from each animal. Statistical analyses were performed with SigmaPlot and data were analyzed by Student's *t* test, with $p < 0.05$ considered to indicate statistically significant differences.

RESULTS

Ca^{2+}-independent, Microcystin-induced LC_{20} Diphosphorylation and Contraction—Fig. 1*A* show the time course of Ca^{2+}-independent contraction of Triton-skinned rat caudal arterial smooth muscle strips in response to the phosphatase inhibitor microcystin ($t_{½}$ = 451.1 ± 13.4 s (n = 8)). Tissues were immersed in TCA/acetone/DTT at the indicated times during the contractile response, washed with acetone, lyophilized, and tissue proteins were extracted in SDS gel sample buffer. Phosphorylated and unphosphorylated forms of LC_{20} were separated by Phos-tag SDS-PAGE (49) and detected by Western blotting with anti-pan LC_{20}, which recognizes all forms of the protein (Fig. 1*B*, *panel a*). The three separated bands were identified by Western blotting with phosphospecific antibodies to LC_{20} (Fig. 1*B*, *panels b-d*). In resting tissue in the absence of Ca^{2+} (*lane 1*), only unphosphorylated LC_{20} was detected. Treatment with microcystin in the absence of Ca^{2+} induced a time-dependent increase in mono- and diphosphorylated LC_{20}. The monophosphorylated band contained a mixture of LC_{20} phosphorylated exclusively at Ser^{19} (Fig. 1*B*, *panel b*) and LC_{20} phosphorylated exclusively at Thr^{18} (Fig. 1*B*, *panel c*). The antibody to $Thr(p)^{18}$-LC_{20} also recognized diphosphorylated LC_{20} (Fig. 1*B*, *panel c*), identified as containing both $Thr(P)^{18}$ and $Ser(P)^{19}$ in Fig. 1*B*, *panel d*. The cumulative quantitative data in Fig. 1*C* show the time-dependent increase in mono- and diphosphorylation, and the corresponding decrease in unphosphorylated LC_{20} in response to microcystin in the absence of Ca^{2+}.

Ca^{2+}-independent, Calyculin-A-induced LC_{20} Diphosphorylation and Contraction—Treatment of intact rat caudal arterial smooth muscle with the membrane-permeant phosphatase inhibitor calyculin-A in Ca^{2+}-free solution also induced LC_{20} mono- and diphosphorylation, which correlated with force development with a $t_{½}$ of 1326 ± 96 s (n = 6) (Fig. 2). In this case, the amount of monophosphorylated LC_{20} detected was significantly less (Fig. 2*C*) than was observed in the Triton-skinned tissue in response to microcystin (Fig. 1*C*). It is also noteworthy that the steady-state force achieved in response to calyculin-A in the absence of Ca^{2+} appeared to be significantly higher than the force induced by a strong depolarizing stimulus (87 mM KCl) (Fig. 2*A*). This prompted us to address the question: does LC_{20} diphosphorylation elicit more steady-state isometric force than monophosphorylation?

KCl-induced LC_{20} Monophosphorylation and Contraction—We first demonstrated that an increase in cytosolic free Ca^{2+} concentration induced exclusively monophosphorylation of LC_{20} at Ser^{19}. Ca^{2+} entry via voltage-gated Ca^{2+} channels was activated by KCl-induced membrane depolarization of intact rat caudal arterial smooth muscle strips, which induced a rapid contractile response ($t_{½}$ = 10.2 ± 0.2 s (n = 29)) (Fig. 3*A*). Analysis of the LC_{20} phosphorylation time course revealed phosphorylation at Ser^{19} (Fig. 3*B*, *panel b*) with no phosphorylation at Thr^{18} (Fig. 3*B*, *panel c*) or diphosphorylation at Thr^{18} and Ser^{19} (Fig. 3*B*, *panels a* and *d*). LC_{20} phosphorylation stoichiometry peaked at ~0.6 mol of P_i/mol of LC_{20} (Fig. 3*C*).

Effects on Force and LC_{20} Phosphorylation of Sequential Treatment with Ca^{2+} and Microcystin—Similarly, addition of Ca^{2+} to Triton-skinned rat caudal arterial smooth muscle induced phosphorylation of LC_{20} exclusively at Ser^{19} (Fig. 4*G*, *lanes A* in *panels a-d*) with a $t_{½}$ of 151.7 ± 4.8 s (n = 23) and an LC_{20} phosphorylation level of ~0.5 mol of P_i/mol of LC_{20} (Table 1). Addition of microcystin at the plateau of a Ca^{2+}-induced contraction resulted in a further increase in force of ~25% (Fig. 4*B* and Table 2), which correlated with LC_{20} diphosphorylation (Fig. 4*G*, *lanes B* in *panels a–d*, and Table 1). If microcystin and Ca^{2+} were added together, a rapid contraction occurred ($t_{½}$ of 65.3 ± 2.3 s (n = 15) compared with 151.7 ± 4.8 s (n = 23) for Ca^{2+} alone and 451.1 ± 13.4 s (n = 8) for microcystin at *p*Ca 9), which was again accompanied by LC_{20} diphosphorylation (Fig. 4*G*, *lanes C* in *panels a–d*, and Table 1).

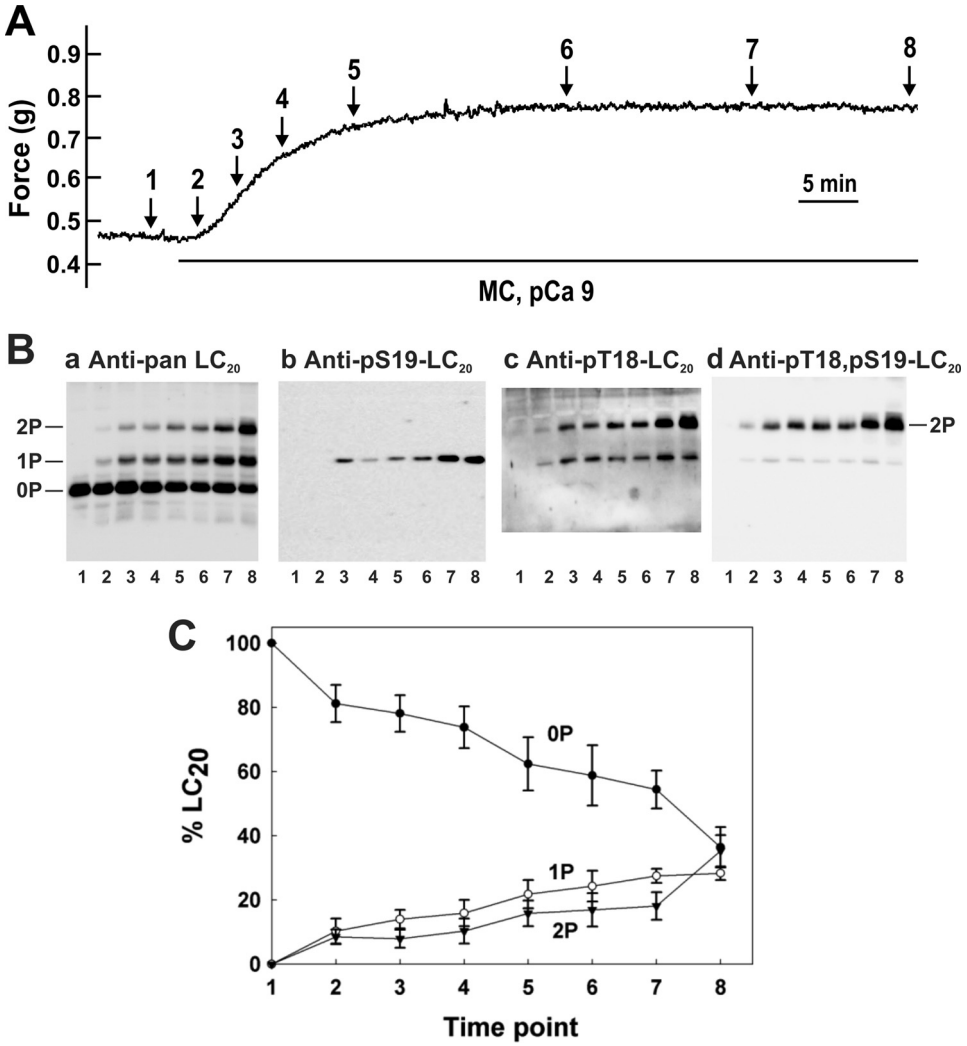

FIGURE 1. **Ca^{2+}-independent contraction and LC_{20} diphosphorylation in Triton-skinned rat caudal arterial smooth muscle in response to microcystin at *p*Ca 9.** *A,* Triton-skinned rat caudal arterial smooth muscle strips mounted on a force transducer in *p*Ca 9 solution were treated with microcystin (1 μM). A typical contractile response is shown. Separate tissues were harvested at the indicated times during the contraction for analysis of LC_{20} phosphorylation by Phos-tag SDS-PAGE and Western blotting (*B*) with antibodies to LC_{20} (*panel a*), $Ser(P)^{19}$-LC_{20} (*panel b*), $Thr(P)^{18}$-LC_{20} (*panel c*), and $Thr(P)^{18}$,$Ser(P)^{19}$-LC_{20} (*panel d*). *Numbers below* the gel lanes correspond to the time points in *A*. *C,* cumulative quantitative data showing the proportions of unphosphorylated (*0P*, *closed circles*), mono- (*1P*, *open circles*), and diphosphorylated LC_{20} (*2P*, *closed inverted triangles*) as a function of time. Values represent the mean ± S.E. (n = 3).

No force development or LC_{20} phosphorylation was observed in the absence of Ca^{2+} and phosphatase inhibitor (Fig. 4, *D* and *G*, *lanes D* in *panels a–d*, and Table 1). If contraction was evoked by addition of microcystin in the absence of Ca^{2+}, subsequent addition of Ca^{2+} elicited further force development (~20%; Fig. 4*F* and Table 2) and LC_{20} diphosphorylation (Fig. 4*G*, *lanes F* in *panels a–d*, and Table 1) compared with control (Fig. 4, *E* and *G*, *lanes E*, and Tables 1 and 2). A more detailed analysis of the (Ca^{2+} + microcystin)-induced contraction revealed rapid phosphorylation of LC_{20} at Ser^{19} that can be attributed to MLCK activation by Ca^{2+}, and a slower rate of phosphorylation at Thr^{18}, due to ILK activity that is unmasked by the phosphatase inhibitor (Fig. 5).

Effects on Force and LC_{20} Phosphorylation of Combined Treatment with KCl and Calyculin-A—Calyculin-A treatment of intact rat caudal arterial smooth muscle in the presence of extracellular Ca^{2+} elicited a slow, sustained contraction (Fig. 6, *green trace*) with a $t_{½}$ of 1206 ± 102 s (n = 6), which was indistinguishable from the calyculin-A-induced contraction in Ca^{2+}-free solution ($t_{½}$ = 1326 ± 96 s (n = 6)) (Fig. 2*A*). Membrane depolarization in the presence of extracellular Ca^{2+} elicited a rapid increase in force ($t_{½}$ = 10.2 ± 0.2 s (n = 29)), which subsequently declined to a steady-state level (Figs. 3*A* and 6, *red trace*). The simultaneous application of KCl and calyculin-A in the presence of extracellular Ca^{2+} elicited a contractile response (Fig. 6, *black trace*) that matched the superimposed contractions due to membrane depolarization (Fig. 6, *red trace*) and phosphatase inhibition (Fig. 6, *green trace*): the initial rapid contractile response in the presence of KCl and calyculin-A occurred with a $t_{½}$ of 11.2 ± 0.6 s (n = 6), *i.e.* similar to the contraction induced by KCl treatment alone ($t_{½}$ = 10.2 ± 0.2 s (n = 29)), whereas the slow, sustained contractile response occurred with a $t_{½}$ of 1110 ± 84 s (n = 3), *i.e.* similar to the contraction induced by calyculin-A in Ca^{2+}-free solution ($t_{½}$ = 1326 ± 96 s (n = 6)). We hypothesize that the biphasic contractile response to KCl and calyculin-A involves two distinct mechanisms: the rapid response is attributable to membrane depolarization-mediated Ca^{2+} entry and MLCK activation, and

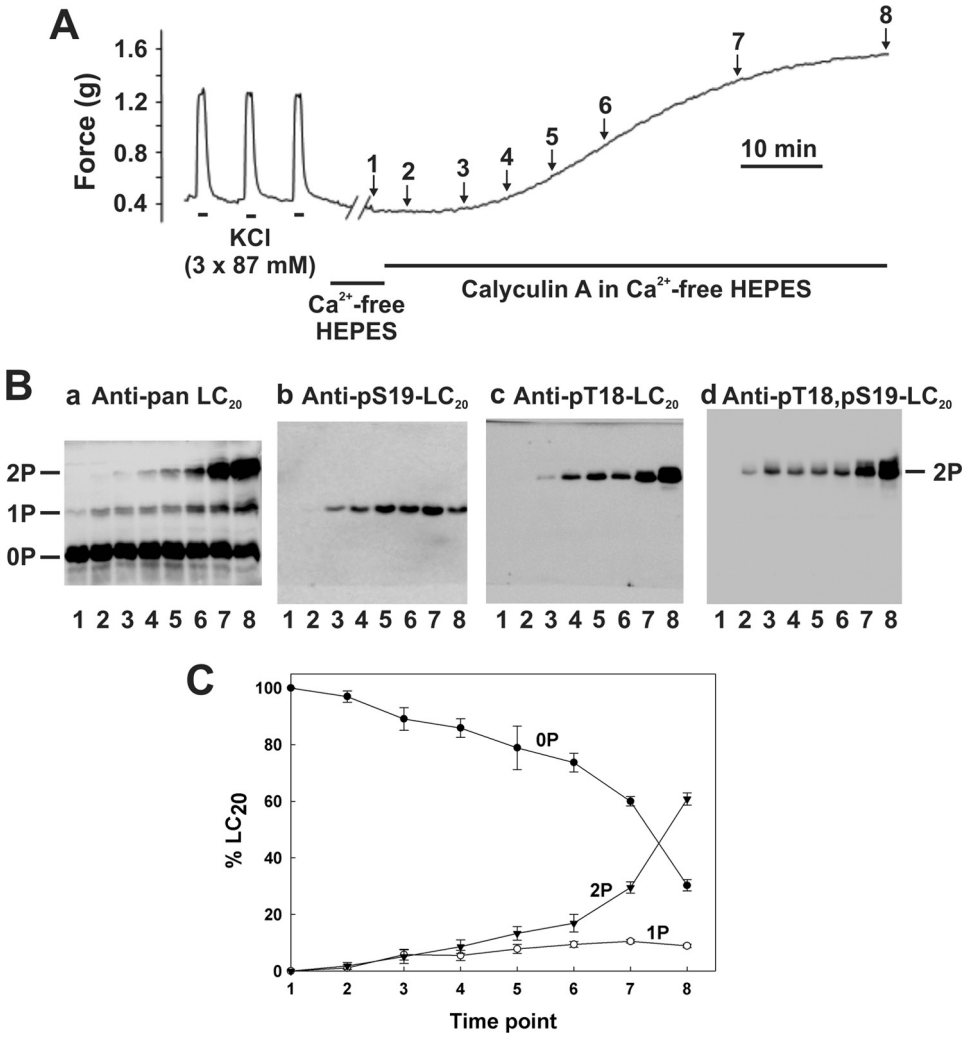

FIGURE 2. **Ca^{2+}-independent contraction and LC_{20} diphosphorylation in intact rat caudal arterial smooth muscle in response to calyculin-A in Ca^{2+}-free solution.** *A,* intact rat caudal arterial smooth muscle strips mounted on a force transducer in Ca^{2+}-containing H-T buffer were induced to contract 3 times with 87 mM KCl. The tissue was then washed extensively with Ca^{2+}-free H-T buffer (which emptied intracellular Ca^{2+} stores because the contractile response to caffeine was abolished; data not shown) prior to treatment with calyculin-A (0.5 μM) in Ca^{2+}-free solution. Separate tissues were harvested at the indicated times during the contraction for analysis of LC_{20} phosphorylation by Phos-tag SDS-PAGE and Western blotting (*B*) with antibodies to LC_{20} (*panel a*), $Ser(P)^{19}$-LC_{20} (*panel b*), $Thr(P)^{18}$-LC_{20} (*panel c*), and $Thr(P)^{18}$,$Ser(P)^{19}$-LC_{20} (*panel d*). *Numbers below* the gel lanes correspond to the time points in *A*. *C,* cumulative quantitative data showing the proportions of unphosphorylated (*0P*, *closed circles*), mono- (*1P*, *open circles*), and diphosphorylated LC_{20} (*2P*, *closed inverted triangles*) as a function of time. Values represent the mean ± S.E. ($n = 3$).

the slow response to calyculin-A-mediated inhibition of MLCP with unmasking of Ca^{2+}-independent LC_{20} kinase activity. These mechanisms are supported by measurements of site-specific LC_{20} phosphorylation during the time course of contraction in the presence of extracellular Ca^{2+} and following addition of both KCl and calyculin-A (Fig. 7). Thus, there was a rapid initial increase in LC_{20} monophosphorylation (Fig. 7*B*, *panel a*), which occurred exclusively at Ser^{19} (Fig. 7*B*, *panels b* and *c*), followed by a slight dephosphorylation (Fig. 7*C*) leading to partial relaxation (Fig. 7*A*). It was only at prolonged incubation times that diphosphorylation of LC_{20} was observed (Fig. 7*B*, *panels a* and *d*), which correlated with the slow, sustained phase of contraction (Fig. 7*A*).

Stoichiometric Phosphorylation of LC_{20} at Ser^{19} in Triton-skinned Tissue—The results described above suggest that phosphorylation of LC_{20} at Thr^{18} may increase the level of force that is achieved in intact or Triton-skinned rat caudal arterial smooth muscle as a result of Ser^{19} phosphorylation. Alternatively, the observed increases in force could be due to an increase in the total level of Ser^{19} phosphorylation, rather than phosphorylation at Thr^{18}. To distinguish between these possibilities, it would be necessary to achieve stoichiometric phosphorylation exclusively at Ser^{19} and then observe whether or not phosphorylation at Thr^{18} has an additional effect on steady-state force. The next step, therefore, was to achieve stoichiometric phosphorylation exclusively at Ser^{19}. Unfortunately, treatment of intact tissue with an optimal KCl concentration to elicit a maximal increase in $[Ca^{2+}]_i$, leading to maximal activation of MLCK, does not lead to stoichiometric phosphorylation of LC_{20} at Ser^{19} (Fig. 3). This is due to competing dephosphorylation of LC_{20} by MLCP, which is constitutively active. Likewise, in Triton-skinned tissue, addition of a maximal $[Ca^{2+}]$ fails to elicit stoichiometric LC_{20} phosphorylation at Ser^{19} for the same reason (Fig. 4*G*, *lane A* in *panel a*, and Table 1). We tested the possibility that the stoichiometry of LC_{20} phosphorylation could be increased by addition of exogenous calmodu-

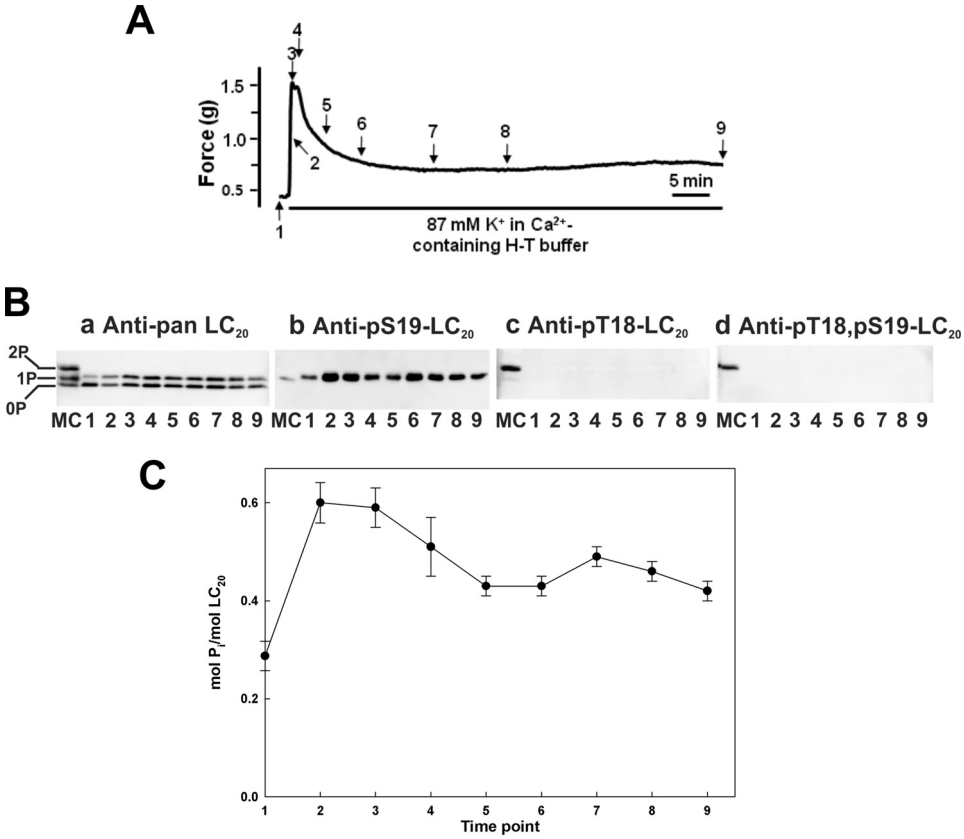

FIGURE 3. **Contraction and LC_{20} phosphorylation in intact rat caudal arterial smooth muscle in response to KCl-induced depolarization in the presence of Ca^{2+}.** *A*, intact rat caudal arterial smooth muscle strips were treated with 87 mM KCl in Ca^{2+}-containing H-T buffer and the contractile response was recorded. Separate tissues were harvested at the indicated times during the contraction for analysis of LC_{20} phosphorylation by Phos-tag SDS-PAGE and Western blotting with antibodies to LC_{20} (*panel a*), Ser(P)^{19}-LC_{20} (*panel b*), Thr(P)^{18}-LC_{20} (*panel c*), and Thr(P)^{18},Ser(P)^{19}-LC_{20} (*panel d*). *Numbers below* the gel lanes correspond to the time points in *A*. *MC* denotes control tissue (Triton-skinned rat caudal arterial smooth muscle treated with microcystin at pCa 9 for 60 min) to identify unphosphorylated, mono-, and diphosphorylated LC_{20} bands. *C*, cumulative quantitative data showing the time course of LC_{20} phosphorylation stoichiometry; as shown in *panel b*, phosphorylation occurred exclusively at Ser^{19} under these conditions. Values represent the mean ± S.E. ($n = 3$).

lin and MLCK to Triton-skinned tissue in the presence of Ca^{2+}, recognizing the caveat that, if the MLCK concentration was too high, it would phosphorylate Thr^{18} as well. Whereas the addition of calmodulin in the absence or presence of MLCK did increase LC_{20} phosphorylation slightly, there remained a significant amount of unphosphorylated LC_{20}, and a low level of LC_{20} diphosphorylation was observed (supplemental Fig. S1 and Table S1). This approach was, therefore, unsuitable for achieving stoichiometric phosphorylation at Ser^{19} in the absence of Thr^{18} phosphorylation.

An alternative approach to achieve stoichiometric LC_{20} phosphorylation was to use ATPγS to thiophosphorylate LC_{20}: MLCK uses ATPγS as a substrate (50), but the thiophosphorylated protein is not a substrate for MLCP (51). This approach was used successfully with Triton-skinned rat caudal arterial smooth muscle (Fig. 8). Triton-skinned tissues were shown to be viable by contraction at *p*Ca 4.5 in the presence of ATP and an ATP regenerating system, and relaxation following removal of Ca^{2+} (Fig. 8*A*). Following removal of ATP, incubation with ATPγS in the presence of Ca^{2+}, but absence of ATP or an ATP regenerating system, resulted in stoichiometric thiophosphorylation of LC_{20} at Ser^{19} (Fig. 8*B*, *lanes 2* and *3*). It is noteworthy that thiophosphorylated LC_{20} migrates more rapidly upon Phos-tag SDS-PAGE than does phosphorylated LC_{20}, which enables clear discrimination between phosphorylated and thiophosphorylated forms of the protein.

ATPγS is not hydrolyzed by activated myosin and therefore does not support cross-bridge cycling and contraction (20, 52, 53). Stoichiometric thiophosphorylation at Ser^{19} (Fig. 8*B*, *lanes 2* and *3*) was, therefore, not accompanied by contraction (Fig. 8*A*). Transfer to *p*Ca 9 solution containing ATP and an ATP regenerating system following washout of ATPγS resulted in a rapid contractile response ($t_{1/2}$ = 21.2 ± 0.2 s ($n = 8$)) and steady-state force corresponding to 85.4 ± 1.9% ($n = 8$) of the *p*Ca 4.5-induced contraction (Fig. 8*A*). Once the steady-state force was achieved, microcystin was added at *p*Ca 9 in the presence of ATP and an ATP regenerating system. No additional force development was observed (77.3 ± 4.2% ($n = 5$) of *p*Ca 4.5-induced contraction), although significant di(thio)phosphorylation of LC_{20} did occur (Fig. 8*B*, *lanes 6* and *7*, and Table 3).

The identities of the thiophosphorylated LC_{20} species as depicted in Fig. 8*B* were verified by the use of phosphospecific antibodies (supplemental Fig. S2). Incubation of Triton-skinned rat caudal arterial smooth muscle strips with ATPγS and microcystin at *p*Ca 9, in the absence of ATP and an ATP regenerating system, failed to elicit thiophosphorylation of LC_{20} (supplemental Fig. S3, *lanes 3* and *4*). This is in contrast to

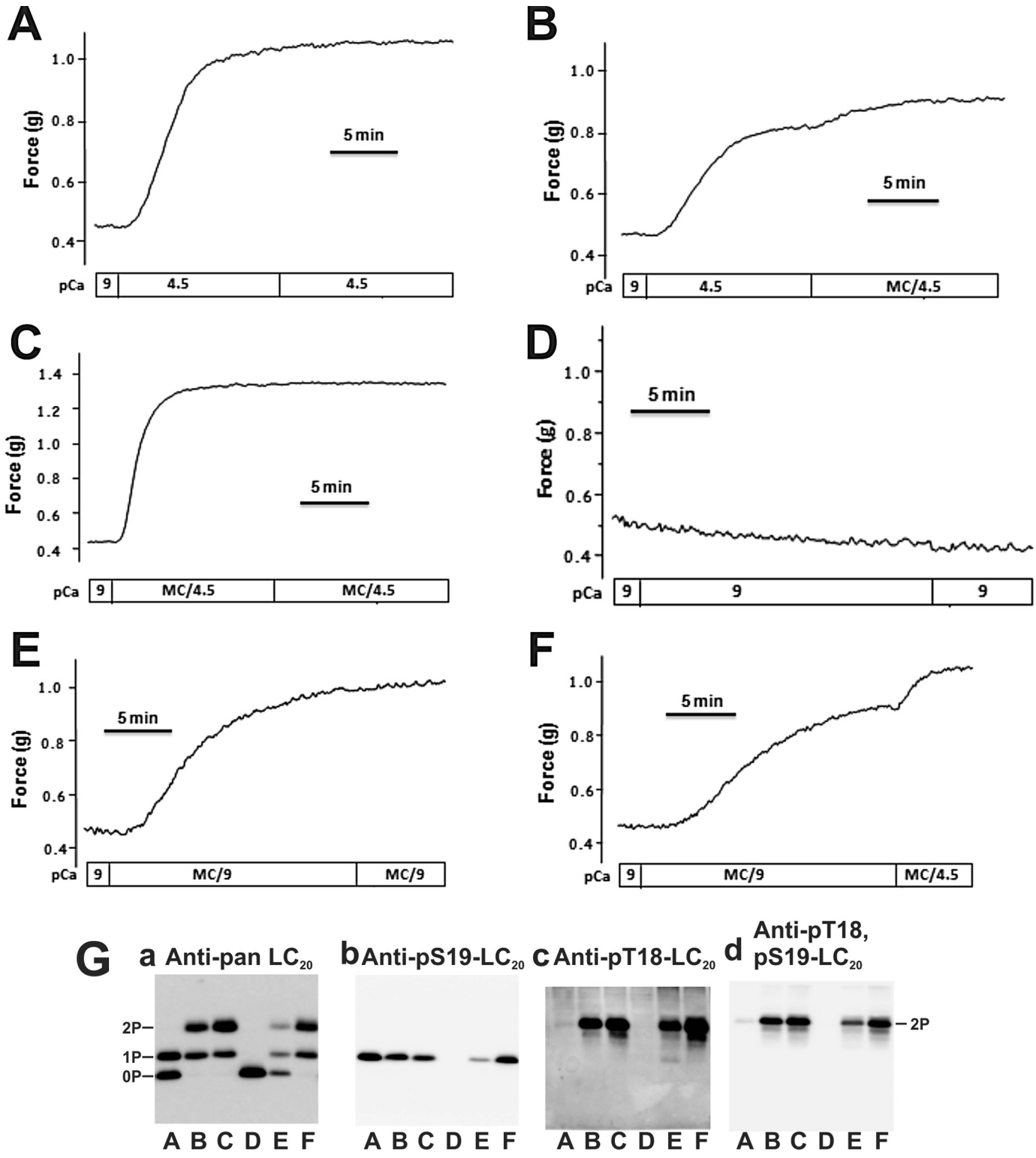

FIGURE 4. **Effect of microcystin on Ca^{2+}-induced contraction and Ca^{2+} on microcystin-induced contraction of Triton-skinned rat caudal arterial smooth muscle.** *A–F,* Triton-skinned rat caudal arterial smooth muscle strips mounted on a force transducer in *p*Ca 9 solution were treated as indicated. *G,* LC_{20} phosphorylation at the end of the protocols shown in *A–F* was analyzed by Phos-tag SDS-PAGE and Western blotting with antibodies to LC_{20} (*panel a*), $Ser(P)^{19}$-LC_{20} (*panel b*), $Thr(P)^{18}$-LC_{20} (*panel c*), and $Thr(P)^{18}$,$Ser(P)^{19}$-LC_{20} (*panel d*). *Letters below* the gel lanes correspond to *panels A–F*. Results are representative of at least 3 independent experiments.

incubation with ATPγS at *p*Ca 4.5, in the absence of ATP and an ATP regenerating system, which led to LC_{20} monothiophosphorylation (supplemental Fig. S3, *lane 2*) at Ser^{19} (supplemental Fig. S2, *lanes 3–5*).

Effects of Diphosphorylation of LC_{20} on the Rates of Dephosphorylation and Relaxation—Finally, we investigated the possibility that LC_{20} diphosphorylation may affect relaxation, rather than contraction, by comparing the rates of dephospho-

TABLE 1

Quantification of LC_{20} mono- and diphosphorylation in Triton-skinned rat caudal arterial smooth muscle

LC_{20} phosphorylation levels were quantified by Phos-tag SDS-PAGE (see Fig. 4*G*, *panel a*) in tissues treated as described in the legend to Fig. 4, *A–F*. Values indicate the levels of unphosphorylated (0P), monophosphorylated (1P), and diphosphorylated LC_{20} (2P) under the conditions indicated.

Conditions	% Total LC_{20}			*n*
	0P	1P	2P	
*p*Ca4.5/*p*Ca 4.5	52.1 ± 3.2	47.9 ± 3.2	0	4
*p*Ca 4.5/MC, *p*Ca 4.5	0	40.3 ± 2.6	59.6 ± 2.7	5
MC, *p*Ca 4.5/MC, *p*Ca 4.5	0	27.8 ± 3.8	71.0 ± 4.3	4
*p*Ca 9/*p*Ca 9	100	0	0	3
MC, *p*Ca 9/MC, *p*Ca 9	41.7 ± 3.1	30.6 ± 2.5	27.7 ± 2.5	5
MC, *p*Ca 9/MC, *p*Ca 4.5	0	34.3 ± 4.3	64.4 ± 4.6	5

TABLE 2

The effects on steady-state isometric force of sequential treatment of Triton-skinned rat caudal arterial smooth muscle with Ca^{2+} and microcystin

Steady-state force measurements were made under the conditions indicated in the legend to Fig. 4, *A–F*. Values of Force (%) indicate the levels of steady-state force at the end of the protocol compared to that before transfer to the final bathing solution. For example, in the case of Fig. 4*B*, where the tissue was contracted with *p*Ca 4.5 and then transferred to *p*Ca 4.5 solution containing microcystin, steady-state force in the presence of Ca^{2+} and microcystin was 124.5 ± 2.2% of that in the presence of Ca^{2+} alone.

Conditions	Force (%)	*n*
*p*Ca 4.5/*p*Ca 4.5	105.1 ± 1.4	4
*p*Ca 4.5/MC, *p*Ca 4.5	124.5 ± 2.2	5
MC, *p*Ca 4.5/MC, *p*Ca 4.5	100.8 ± 0.3	4
MC, *p*Ca 9/MC, *p*Ca9	106.1 ± 1.8	4
MC, *p*Ca 9/MC, *p*Ca 4.5	121.4 ± 3.0	5

rylation and relaxation of Triton-skinned rat caudal arterial smooth muscle following monophosphorylation of LC_{20} at *p*Ca 4.5 or diphosphorylation of LC_{20} at *p*Ca 9 in the presence of okadaic acid. Okadaic acid was chosen as the phosphatase inhibitor for these experiments, rather than microcystin, because its effects are readily reversible (54), whereas microcystin can covalently modify the catalytic subunit of type 1 protein phosphatase, resulting in irreversible inhibition of the phosphatase (55). Indeed, we have observed that microcystin-induced contractions cannot be reversed by washout of the inhibitor (data not shown).

Comparable levels of phosphorylation of LC_{20} were achieved with *p*Ca 4.5 (0.48 ± 0.02 mol of P_i/mol of LC_{20} ($n = 4$)) or okadaic acid treatment at *p*Ca 9 (0.49 ± 0.09 mol of P_i/mol of LC_{20} ($n = 5$)), with monophosphorylation occurring exclusively in response to Ca^{2+} and both mono- and diphosphorylation being detected in the presence of okadaic acid, as expected (Fig. 9*C*). The steady-state force generated by okadaic acid at *p*Ca 9 was 83.3 ± 1.4% ($n = 9$) of that at *p*Ca 4.5 (supplemental Fig. S4). Relaxation was initiated by transfer to *p*Ca 9 solution and the time courses of LC_{20} dephosphorylation and relaxation were quantified (Fig. 9, *A* and *B*, respectively). The rate of dephosphorylation of LC_{20} was markedly reduced in the tissues in which LC_{20} had been diphosphorylated compared with tissues containing exclusively monophosphorylated LC_{20} (Fig. 9*A*): $t_{1/2}$ values were 83.3 s for Ca^{2+}-treated tissue and 560 s for okadaic acid-treated tissue. This correlated with a reduction in the rate of relaxation (Fig. 9*B*): $t_{1/2}$ values were 560 s for Ca^{2+}-treated tissue and 1293 s for okadaic acid-treated tissue. The slower rate of dephosphorylation following okadaic acid treatment cannot be explained by slow washout of the inhibitor because MYPT1-Thr^{697} and -Thr^{855} (the inhibitory phosphorylation sites in the myosin targeting subunit of MLCP) (56) were maximally dephosphorylated at the first time point analyzed during the relaxation, *i.e.* when force was at 90% (supplemental Fig. S5).

DISCUSSION

LC_{20} diphosphorylation has been observed in several smooth muscle tissues treated with various contractile stimuli, including carbachol- (37) and neurally stimulated bovine tracheal smooth muscle (38), prostaglandin-$F_{2\alpha}$-stimulated rabbit thoracic aorta (39, 40), and angiotensin II-stimulated rat renal efferent arterioles (41). LC_{20} diphosphorylation has also been observed in pathological cases of smooth muscle hypercontractility, for example, coronary artery spasm (44, 45), cerebral vasospasm after subarachnoid hemorrhage (43, 46), and intimal hyperplasia (42). More recently, Cho *et al.* (57) provided evidence for enhanced Ca^{2+}-independent LC_{20} diphosphorylation and force generation in β-escin-permeabilized mesenteric arterial smooth muscle rings of spontaneously hypertensive rats compared with normotensive Wistar Kyoto controls. Furthermore, phenylephrine induced significant LC_{20} diphosphorylation in the spontaneously hypertensive rat arteries. Evidence was also presented that ZIPK contributes to the Ca^{2+}-independent LC_{20} diphosphorylation through phosphorylation of MYPT1 at Thr^{697} and possibly direct phosphorylation of LC_{20}, and the expression level of ZIPK, but not ILK, was greater in spontaneously hypertensive rats than Wistar Kyoto tissues (57). Collectively, these data suggest that LC_{20} diphosphorylation may account for the hypercontractility observed in smooth muscle tissues in response to certain contractile stimuli and in pathological situations. It was, therefore, important to determine the functional effect of LC_{20} phosphorylation on smooth muscle contractility. The results of these studies led to the following conclusions.

(i) Treatment of Triton-skinned rat caudal arterial smooth muscle with the phosphatase inhibitor microcystin in the absence of Ca^{2+} induced a slow, sustained contraction, as previously observed (16), which correlated with LC_{20} phosphorylation at Ser^{19} and Thr^{18} (Fig. 1).

(ii) Similar results were obtained when intact tissues were treated with the membrane-permeant phosphatase inhibitor calyculin-A in the absence of extracellular and stored Ca^{2+} (Fig. 2). However, an interesting difference between the Triton-skinned and intact tissues was observed: microcystin treatment of skinned tissue induced monophosphorylation at Ser^{19} and Thr^{18} at similar rates (Fig. 1*B*, *panels b* and *c*), in addition to diphosphorylation (Fig. 1*B*, *panel d*), whereas no monophosphorylation was observed at Thr^{18} following calyculin-A treatment of intact tissue in the absence of extracellular Ca^{2+} (Fig. 2*B*, *panel c*), but instead Ser^{19} monophosphorylation was followed by Thr^{18} phosphorylation to form the diphosphorylated species (Fig. 2*B*). This suggests that LC_{20} phosphorylation at the two sites was random in the Triton-skinned tissue experiments but sequential in the intact tissue experiments. A possible explanation would be that distinct kinases are involved in the two situations, the most likely candidates being ILK and ZIPK, and we have provided evidence that ILK is responsible for

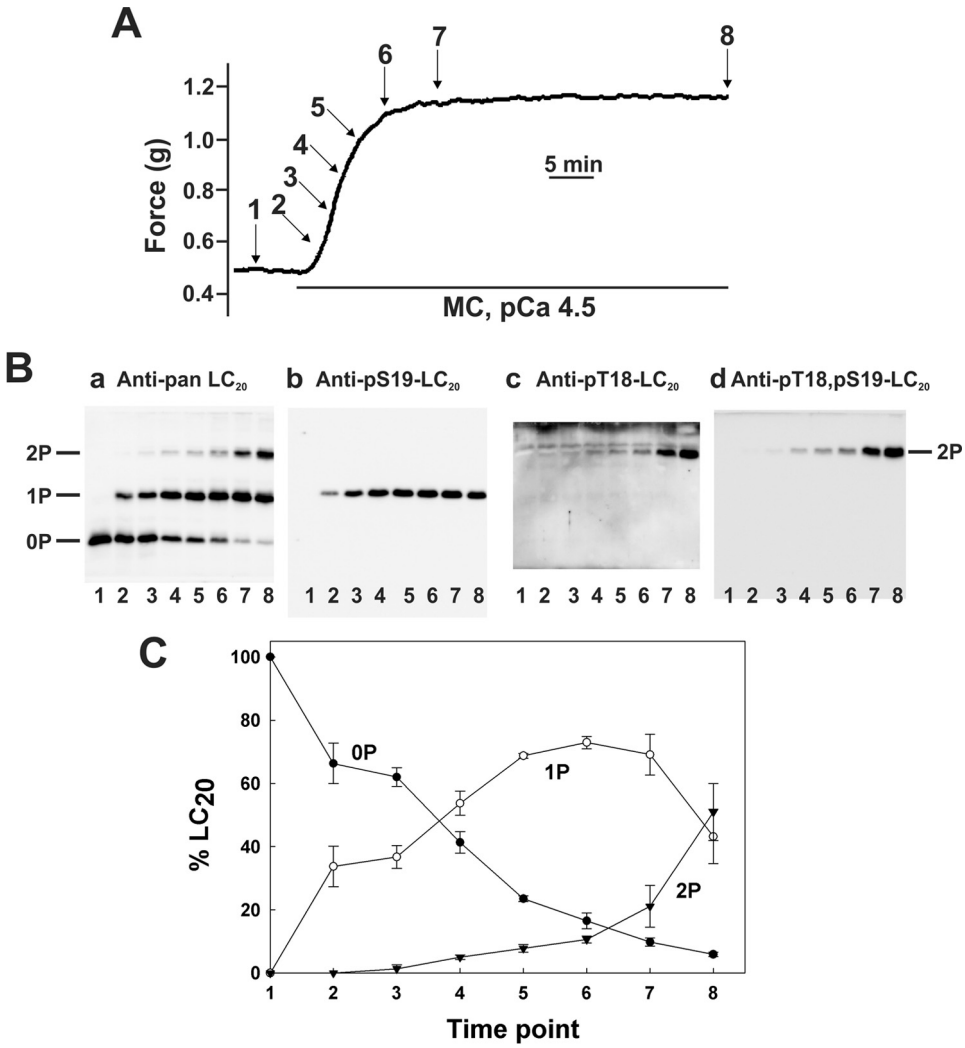

FIGURE 5. **Contraction and LC_{20} diphosphorylation in Triton-skinned rat caudal arterial smooth muscle in response to microcystin at *p*Ca 4.5.** *A*, Triton-skinned rat caudal arterial smooth muscle strips mounted on a force transducer in *p*Ca 9 solution were treated with microcystin (1 μM) at *p*Ca 4.5. Separate tissues were harvested at the indicated times during the contraction for analysis of LC_{20} phosphorylation by Phos-tag SDS-PAGE and Western blotting (*B*) with antibodies to LC_{20} (*panel a*), $Ser(P)^{19}$-LC_{20} (*panel b*), $Thr(P)^{18}$-LC_{20} (*panel c*), and $Thr(P)^{18}$,$Ser(P)^{19}$-LC_{20} (*panel d*). *Numbers below* the gel lanes correspond to the time points in *A*. *C*, cumulative quantitative data showing the proportions of unphosphorylated (*0P*, *closed circles*), mono- (*1P*, *open circles*), and diphosphorylated LC_{20} (*2P*, *closed inverted triangles*) as a function of time. Values represent the mean ± S.E. ($n = 3$).

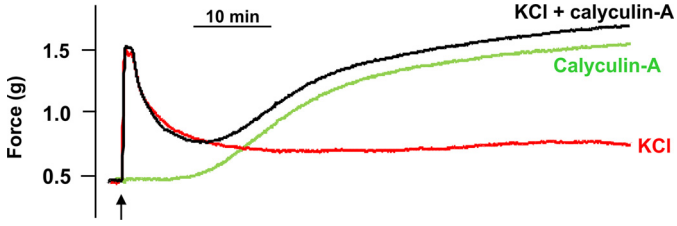

FIGURE 6. **Comparison of the time courses of contraction of intact rat caudal arterial smooth muscle in response to: (i) KCl in the presence of extracellular Ca^{2+}, (ii) calyculin-A in the presence of extracellular Ca^{2+}, and (iii) a combination of KCl and calyculin-A in the presence of extracellular Ca^{2+}.** Membrane-intact rat caudal arterial smooth muscle strips, mounted on a force transducer in Ca^{2+}-containing H-T buffer, were treated with KCl (87 mM) (*red trace*), calyculin-A (0.5 μM) (*green trace*), or both KCl and calyculin-A (*black trace*). The *arrow* indicates the time of application of the contractile stimulus.

microcystin-induced Ca^{2+}-independent contraction of Triton-skinned rat caudal arterial smooth muscle (19).

(iii) The level of steady-state force induced by calyculin-A in the absence of Ca^{2+} is significantly greater than that induced by a maximally effective concentration of KCl, *i.e.* an optimal Ca^{2+} signal (Fig. 2*A*). This would be consistent with diphosphorylation of LC_{20} increasing steady-state force compared with Ser^{19} monophosphorylation. Indeed, addition of microcystin to Triton-skinned tissue pre-contracted at *p*Ca 4.5 (Fig. 4*B*), or of Ca^{2+} to tissue pre-contracted with microcystin in the absence of Ca^{2+} (Fig. 4*F*), evoked a significant increase in steady-state force (Table 2), which correlated with increases in LC_{20} diphosphorylation (Fig. 4*G* and Table 1). However, Ser^{19} phosphorylation stoichiometry also increased under these conditions (from ~0.5 mol of P_i/mol of LC_{20} to ~1 mol of P_i/mol of LC_{20}) (Table 1), suggesting that the enhanced force responses could be due to increased phosphorylation at Ser^{19} (whether in the form of monophosphorylated or diphosphorylated LC_{20}).

(iv) In intact (Fig. 3) and Triton-skinned tissue (Fig. 4*A* and *G*), Ca^{2+} elicited exclusively monophosphorylation of LC_{20} at Ser^{19}, as expected.

(v) The fact that the rate of contraction of Triton-skinned rat caudal arterial smooth muscle in response to Ca^{2+} was signifi-

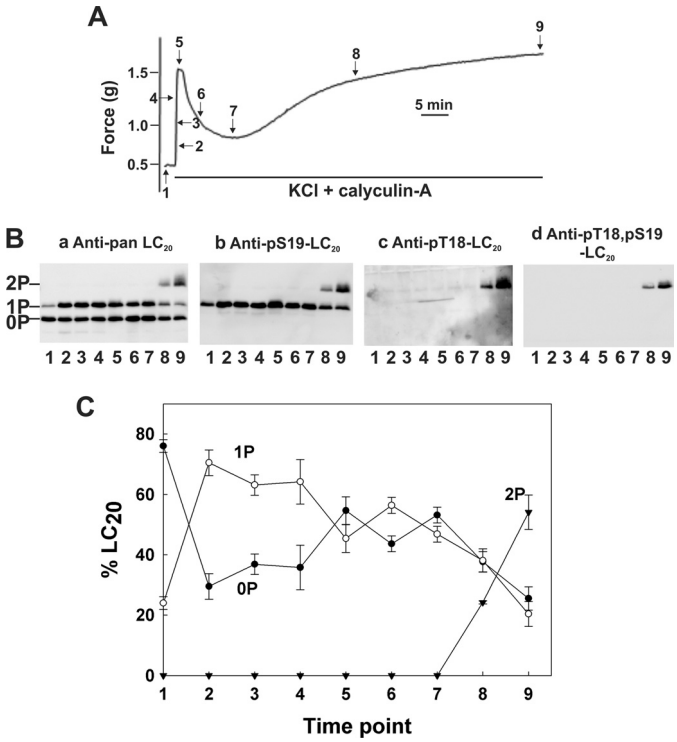

FIGURE 7. **Contraction and LC_{20} diphosphorylation in intact rat caudal arterial smooth muscle in response to KCl and calyculin-A in the presence of extracellular Ca^{2+}.** *A,* membrane-intact rat caudal arterial smooth muscle strips, mounted on a force transducer in Ca^{2+}-containing H-T buffer, were treated with KCl (87 mM) and calyculin-A (0.5 μM). Separate tissues were harvested at the indicated times during the contraction for analysis of LC_{20} phosphorylation by Phos-tag SDS-PAGE and Western blotting (*B*) with antibodies to LC_{20} (*panel a*), Ser(P)^{19}-LC_{20} (*panel b*), Thr(P)^{18}-LC_{20} (*panel c*), and Thr(P)^{18},Ser(P)^{19}-LC_{20} (*panel d*). *Numbers below* the gel lanes correspond to the time points in *A*. *C,* cumulative quantitative data showing the proportions of unphosphorylated (*0P*, *closed circles*), mono- (*1P*, *open circles*), and diphosphorylated LC_{20} (*2P*, *closed inverted triangles*) as a function of time. Values represent the mean ± S.E. ($n = 3$).

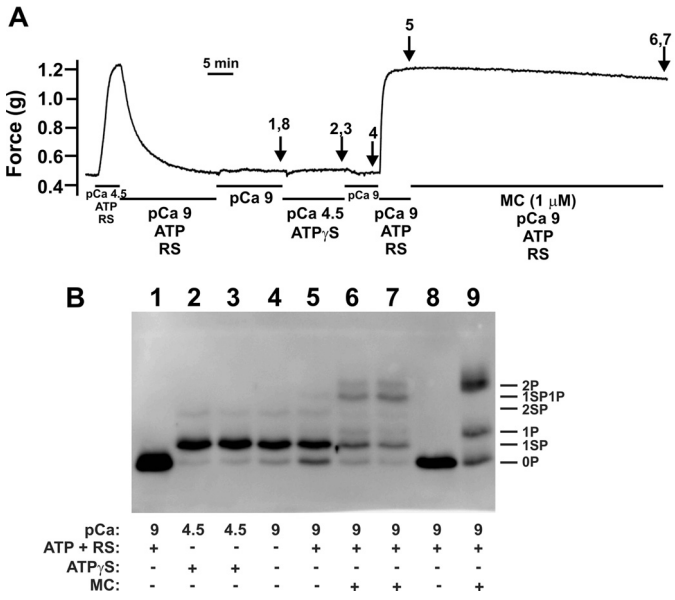

FIGURE 8. **Stoichiometric thiophosphorylation of LC_{20} at Ser^{19} in Triton-skinned rat caudal arterial smooth muscle.** *A,* the viability of Triton-skinned rat caudal arterial smooth muscle strips was initially verified by transfer from relaxing solution (*p*Ca 9) to *p*Ca 4.5 solution containing ATP and an ATP regenerating system (*RS*), which induced a contractile response. Tissues were then relaxed by 3 washes in *p*Ca 9 solution containing ATP and RS. ATP was then removed by 6 washes in *p*Ca 9 solution without ATP or RS. Tissues were then incubated in *p*Ca 4.5 solution containing ATPγS (4 mM) in the absence of ATP and RS. Excess ATPγS was then removed by washing twice with *p*Ca 9 solution without ATP or RS. Contraction was evoked by transfer to *p*Ca 9 solution containing ATP and RS. Once steady-state force was established, microcystin (1 μM) was added in *p*Ca 9 solution containing ATP and RS. Tissues were harvested at the indicated times during this protocol for Phos-tag SDS-PAGE and Western blotting with anti-pan LC_{20} (*B*), as shown by the *arrows* in *A* (the numbers correspond to the lanes in *B*): (i) *lanes 1* and *8,* tissue incubated at *p*Ca 9 showing exclusively unphosphorylated LC_{20}; (ii) *lanes 2* and *3, p*Ca 4.5 + ATPγS in the absence of ATP and RS; (iii) *lane 4, p*Ca 9 in the absence of ATP and RS following thiophosphorylation; (iv) *lane 5,* at the plateau of force development following transfer to *p*Ca 9 solution containing ATP and RS; (v) *lanes 6* and *7,* following treatment with microcystin at *p*Ca 9 in the presence of ATP and RS. An additional control is included in *lane 9*: Triton-skinned tissue treated with microcystin at *p*Ca 9 for 60 min to identify unphosphorylated (*0P*), monophosphorylated (*1P*), and diphosphorylated (*2P*) LC_{20} bands. Thiophosphorylated forms of LC_{20} are indicated as follows: *1SP,* monothiophosphorylated LC_{20}; *2SP,* dithiophosphorylated LC_{20}; *1SP1P*, LC_{20} thiophosphorylated at one site and monophosphorylated at the other. Data are representative of 8 independent experiments.

cantly faster ($t_{½} \sim 150$ s) than that in response to microcystin at *p*Ca 9 ($t_{½} \sim 450$ s) suggested that it may be possible to induce maximal phosphorylation at Ser^{19} before achieving diphosphorylation, and thereby determine more convincingly if diphosphorylation causes additional force development. Furthermore, treatment with microcystin at *p*Ca 4.5 caused a significant increase in the rate of contraction ($t_{½} \sim 65$ s) compared with Ca^{2+} alone ($t_{½} \sim 150$ s) or microcystin alone ($t_{½} \sim 450$ s). Detailed analysis of the (Ca^{2+} + microcystin)-induced contraction of Triton-skinned rat caudal arterial smooth muscle revealed rapid phosphorylation of LC_{20} at Ser^{19} (which can be attributed to MLCK activation by Ca^{2+}) and a slower rate of phosphorylation at Thr^{18} (due to ILK activity that is unmasked by the phosphatase inhibitor) (Fig. 5). The observation that no additional force was evoked as diphosphorylated LC_{20} appeared argues that Thr^{18} phosphorylation likely does not increase steady-state force beyond that achieved by phosphorylation at Ser^{19}.

(vi) The combination of KCl and calyculin-A in the presence of Ca^{2+} induced a biphasic contractile response of intact tissue (Fig. 6), which corresponds to the combined contractile responses to KCl in the presence of Ca^{2+} and calyculin-A in the absence or presence of Ca^{2+}. In this case, the initial rapid phasic contraction correlated with Ser^{19} phosphorylation, and the slow sustained contractile response with the diphosphorylation of LC_{20} (Fig. 7). The contractile effects of KCl and calyculin-A, however, could be explained entirely by Ser^{19} phosphorylation.

It was necessary, therefore, to devise a way to achieve stoichiometric phosphorylation at Ser^{19} without Thr^{18} phosphorylation, and then observe whether subsequent phosphorylation at Thr^{18} has an effect on steady-state force development. This was achieved by using ATPγS to evoke close-to-stoichiometric thiophosphorylation at Ser^{19} with very little dithiophosphorylation (Fig. 8*B* and Table 3). Subsequent phosphorylation of LC_{20} at Thr^{18} (Fig. 8*B*) failed to elicit an increase in force (Fig. 8*A*). We conclude, therefore, that phosphorylation at Ser^{19} of LC_{20} accounts for maximal force development, and no further force results from additional phosphorylation at Thr^{18}.

We then turned our attention to the possibility that diphosphorylation may affect relaxation rather than contraction by comparing the time courses of dephosphorylation of LC_{20} and

TABLE 3

Thiophosphorylation of LC_{20} in Triton-skinned rat caudal arterial smooth muscle

Values represent percentage of total LC_{20} ± S.E. ($n = 3$). *, #, and ∧ indicate values are not statistically significantly different from each other; 0P, unphosphorylated LC_{20}; 1SP, monothiophosphorylated LC_{20}; 1P, monophosphorylated LC_{20}; 1SP1P, LC_{20} thiophosphorylated at one site and phosphorylated at the other; 2P, diphosphorylated LC_{20}; RS, ATP regenerating system; MC, microcystin.

Conditions	0P	1SP	1P	1SP1P	2P
ATPγS, *p*Ca 4.5, no RS	6.0 ± 2.5*	88.4 ± 4.8#	0	0	5.6 ± 4.3∧
Then *p*Ca 9, no RS	11.1 ± 3.4*	81.6 ± 3.9#	0	0	7.2 ± 2.7∧
Then *p*Ca 9, RS	16.6 ± 4.7*	80.0 ± 4.4#	0	0	3.4 ± 1.9∧
Then MC, *p*Ca 9, RS	13.9 ± 3.2	54.7 ± 4.0	3.4 ± 2.1	14.0 ± 9.2	13.9 ± 8.6

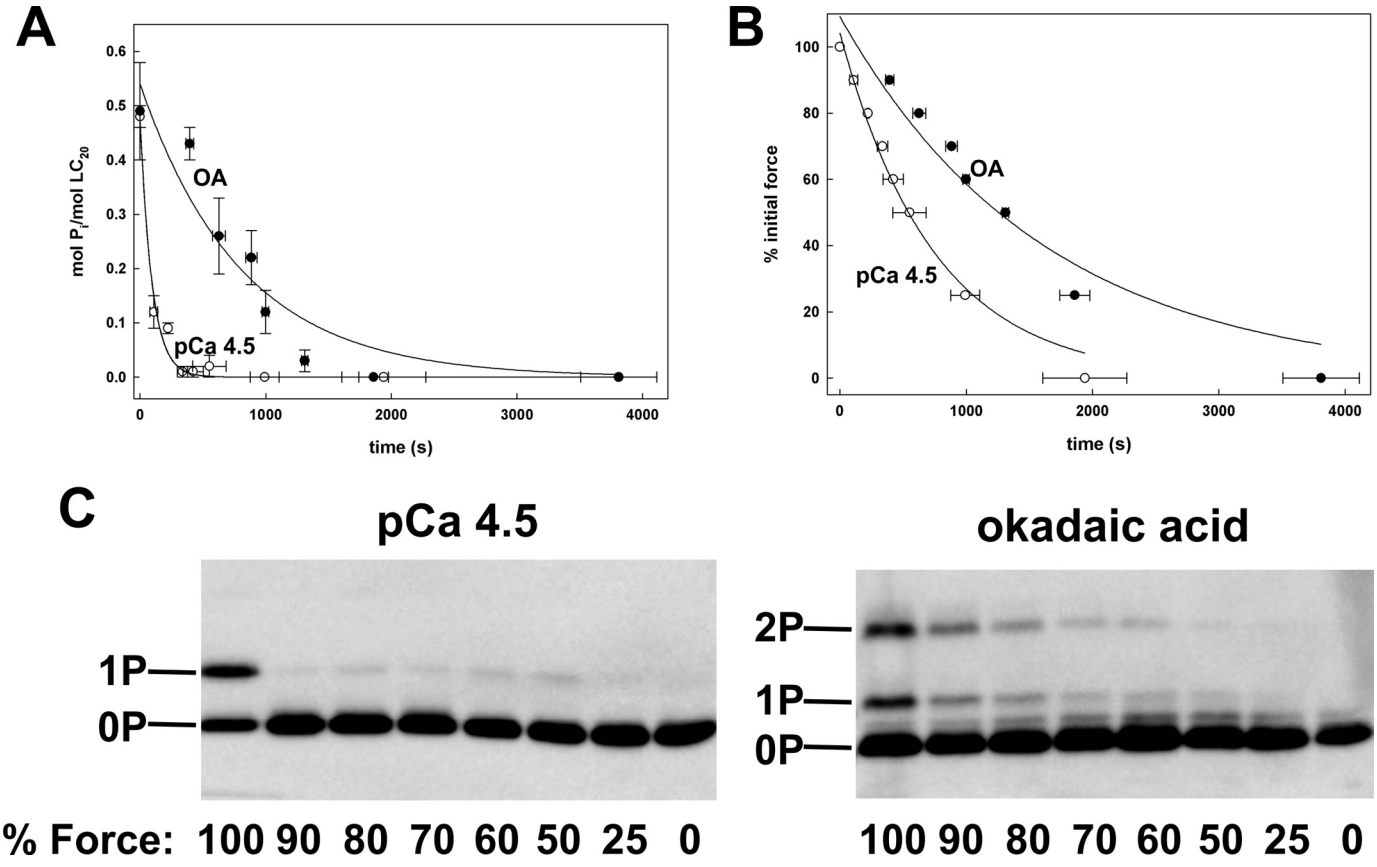

FIGURE 9. **Comparison of the time courses of relaxation and LC_{20} dephosphorylation in Triton-skinned rat caudal arterial smooth muscle following contraction with Ca^{2+} or okadaic acid in the absence of Ca^{2+}.** Triton-skinned tissues that had been contracted with Ca^{2+} (*open circles*) or okadaic acid (20 μM) at *p*Ca 9 (*closed circles*) were transferred to *p*Ca 9 solution and the time courses of dephosphorylation (*A*) and relaxation (*B*) were followed. Tissues were harvested at 10, 20, 30, 40, 50, 75, and 100% relaxation and LC_{20} phosphorylation levels were quantified by Phos-tag SDS-PAGE and Western blotting with anti-pan LC_{20}. Values represent the mean ± S.E. ($n = 5$). Representative Western blots are shown in *C*.

relaxation of Triton-skinned muscle strips that had been pre-contracted under conditions that evoked phosphorylation exclusively at Ser^{19} or at both Ser^{19} and Thr^{18} to the same overall phosphorylation stoichiometry. The rates of dephosphorylation and relaxation were significantly slower in the case of diphosphorylated LC_{20} (Fig. 9). We conclude, therefore, that diphosphorylation of LC_{20} at Thr^{18} and Ser^{19} has a marked effect on relaxation compared with monophosphorylation at Ser^{19}.

The mechanism underlying the reduction in the rate of dephosphorylation of diphosphorylated LC_{20} compared with Ser^{19}-monophosphorylated LC_{20} remains to be determined. A possibility is that the K_m of MLCP for diphosphorylated LC_{20} may be significantly higher than that for LC_{20} phosphorylated exclusively at Ser^{19}. Although such kinetic comparisons have not been performed to date, *in vitro* assays indicated that dephosphorylation of diphosphorylated LC_{20} (whether free or in intact myosin) occurred by a random mechanism, with dephosphorylation at Ser^{19} and Thr^{18} occurring at similar rates (5).

The principal conclusions from this study are: (i) the level of steady-state force is dictated by the level of Ser^{19} phosphorylation and is unaffected by Thr^{18} phosphorylation; and (ii) Thr^{18} phosphorylation reduces the rate of LC_{20} dephosphorylation and relaxation, supporting a sustained contractile response. There is abundant literature indicating that most contractile stimuli elicit phosphorylation exclusively at Ser^{19} and this can be explained by Ca^{2+}-induced activation of MLCK, with or without a modest degree of Ca^{2+} sensitization due to MLCP inhibition (58). Specific stimuli and pathophysiological situations associated with hypercontractility induce LC_{20} diphosphorylation at Thr^{18} and Ser^{19}. This can be explained by

increased MLCP inhibition, unmasking constitutive Ca^{2+}-independent LC_{20} kinase activity (ILK and/or ZIPK), and potentially an increase in activity of Ca^{2+}-independent LC_{20} kinases, leading to an increase in Ser^{19} phosphorylation (force) and Thr^{18} phosphorylation (sustained contraction). ILK and ZIPK are therefore potential therapeutic targets for the treatment of cerebral and coronary vasospasm, intimal hyperplasia, hypertension, and other conditions associated with hypercontractility.

Acknowledgment—We are grateful to Dr. Ryan Mills for helpful comments on the manuscript.

REFERENCES

1. Berridge, M. J. (2008) Smooth muscle cell calcium activation mechanisms. *J. Physiol.* **586,** 5047–5061
2. Allen, B. G., and Walsh, M. P. (1994) The biochemical basis of the regulation of smooth muscle contraction. *Trends Biochem. Sci.* **19,** 362–368
3. Walsh, M. P. (1991) The Ayerst Award Lecture 1990. Calcium-dependent mechanisms of regulation of smooth muscle contraction. *Biochem. Cell Biol.* **69,** 771–800
4. Ikebe, M., and Hartshorne, D. J. (1985) Phosphorylation of smooth muscle myosin at two distinct sites by myosin light chain kinase. *J. Biol. Chem.* **260,** 10027–10031
5. Ikebe, M., Hartshorne, D. J., and Elzinga, M. (1986) Identification, phosphorylation, and dephosphorylation of a second site for myosin light chain kinase on the 20,000-dalton light chain of smooth muscle myosin. *J. Biol. Chem.* **261,** 36–39
6. Hartshorne, D. J., Ito, M., and Erdödi, F. (2004) Role of protein phosphatase type 1 in contractile functions. Myosin phosphatase. *J. Biol. Chem.* **279,** 37211–37214
7. Shibata, S., Ishida, Y., Kitano, H., Ohizumi, Y., Habon, J., Tsukitani, Y., and Kikuchi, H. (1982) Contractile effects of okadaic acid, a novel ionophore-like substance from black sponge, on isolated smooth muscles under the condition of Ca deficiency. *J. Pharmacol. Exp. Ther.* **223,** 135–143
8. Ozaki, H., Ishihara, H., Kohama, K., Nonomura, Y., Shibata, S., and Karaki, H. (1987) Calcium-independent phosphorylation of smooth muscle myosin light chain by okadaic acid isolated from black sponge (*Halichondria okadai*). *J. Pharmacol. Exp. Ther.* **243,** 1167–1173
9. Hirano, K., Kanaide, H., and Nakamura, M. (1989) Effects of okadaic acid on cytosolic calcium concentrations and on contractions of the porcine coronary artery. *Br. J. Pharmacol.* **98,** 1261–1266
10. Ishihara, H., Ozaki, H., Sato, K., Hori, M., Karaki, H., Watabe, S., Kato, Y., Fusetani, N., Hashimoto, K., and Uemura, D. (1989) Calcium-independent activation of contractile apparatus in smooth muscle by calyculin-A. *J. Pharmacol. Exp. Ther.* **250,** 388–396
11. Obara, K., Takai, A., Ruegg, J. C., and de Lanerolle, P. (1989) Okadaic acid, a phosphatase inhibitor, produces a Ca^{2+} and calmodulin-independent contraction of smooth muscle. *Pflügers Arch.* **414,** 134–138
12. Hori, M., Magae, J., Han, Y. G., Hartshorne, D. J., and Karaki, H. (1991) A novel protein phosphatase inhibitor, tautomycin. Effect on smooth muscle. *FEBS Lett.* **285,** 145–148
13. Gong, M. C., Cohen, P., Kitazawa, T., Ikebe, M., Masuo, M., Somlyo, A. P., and Somlyo, A. V. (1992) Myosin light chain phosphatase activities and the effects of phosphatase inhibitors in tonic and phasic smooth muscle. *J. Biol. Chem.* **267,** 14662–14668
14. Suzuki, A., and Itoh, T. (1993) Effects of calyculin A on tension and myosin phosphorylation in skinned smooth muscle of the rabbit mesenteric artery. *Br. J. Pharmacol.* **109,** 703–712
15. Shirazi, A., Iizuka, K., Fadden, P., Mosse, C., Somlyo, A. P., Somlyo, A. V., and Haystead, T. A. (1994) Purification and characterization of the mammalian myosin light chain phosphatase holoenzyme. The differential effects of the holoenzyme and its subunits on smooth muscle. *J. Biol. Chem.* **269,** 31598–31606
16. Weber, L. P., Van Lierop, J. E., and Walsh, M. P. (1999) Ca^{2+}-independent phosphorylation of myosin in rat caudal artery and chicken gizzard myofilaments. *J. Physiol.* **516,** 805–824
17. Deng, J. T., Van Lierop, J. E., Sutherland, C., and Walsh, M. P. (2001) Ca^{2+}-independent smooth muscle contraction. A novel function for integrin-linked kinase. *J. Biol. Chem.* **276,** 16365–16373
18. Niiro, N., and Ikebe, M. (2001) Zipper-interacting protein kinase induces Ca^{2+}-free smooth muscle contraction via myosin light chain phosphorylation. *J. Biol. Chem.* **276,** 29567–29574
19. Wilson, D. P., Sutherland, C., Borman, M. A., Deng, J. T., Macdonald, J. A., and Walsh, M. P. (2005) Integrin-linked kinase is responsible for Ca^{2+}-independent myosin diphosphorylation and contraction of vascular smooth muscle. *Biochem. J.* **392,** 641–648
20. Walsh, M. P., Bridenbaugh, R., Hartshorne, D. J., and Kerrick, W. G. (1982) Phosphorylation-dependent activated tension in skinned gizzard muscle fibers in the absence of Ca^{2+}. *J. Biol. Chem.* **257,** 5987–5990
21. Ngai, P. K., and Walsh, M. P. (1984) Inhibition of smooth muscle actin-activated myosin Mg^{2+}-ATPase activity by caldesmon. *J. Biol. Chem.* **259,** 13656–13659
22. Walsh, M. P. (1985) Limited proteolysis of smooth muscle myosin light chain kinase. *Biochemistry* **24,** 3724–3730
23. Wilson, D. P., Sutherland, C., and Walsh, M. P. (2002) Ca^{2+} activation of smooth muscle contraction. Evidence for the involvement of calmodulin that is bound to the Triton-insoluble fraction even in the absence of Ca^{2+}. *J. Biol. Chem.* **277,** 2186–2192
24. Mita, M., Yanagihara, H., Hishinuma, S., Saito, M., and Walsh, M. P. (2002) Membrane depolarization-induced contraction of rat caudal arterial smooth muscle involves Rho-associated kinase. *Biochem. J.* **364,** 431–440
25. Wickström, S. A., Lange, A., Montanez, E., and Fässler, R. (2010) The ILK/PINCH/parvin complex. The kinase is dead, long live the pseudokinase! *EMBO J.* **29,** 281–291
26. Maydan, M., McDonald, P. C., Sanghera, J., Yan, J., Rallis, C., Pinchin, S., Hannigan, G. E., Foster, L. J., Ish-Horowicz, D., Walsh, M. P., and Dedhar, S. (2010) Integrin-linked kinase is a functional Mn^{2+}-dependent protein kinase that regulates glycogen synthase kinase-3β (GSK-3β) phosphorylation. *PLoS One* **5,** e12356
27. Hannigan, G. E., McDonald, P. C., Walsh, M. P., and Dedhar, S. (2011) Integrin-linked kinase. Not so "pseudo" after all. *Oncogene* **30,** 4375–4385
28. Moffat, L. D., Brown, S. B., Grassie, M. E., Ulke-Lemée, A., Williamson, L. M., Walsh, M. P., and MacDonald, J. A. (2011) Chemical genetics of zipper-interacting protein kinase reveal myosin light chain as a bona fide substrate in permeabilized arterial smooth muscle. *J. Biol. Chem.* **286,** 36978–36991
29. Walsh, M. P. (2011) Vascular smooth muscle myosin light chain diphosphorylation. Mechanism, function, and pathological implications. *IUBMB Life* **63,** 987–1000
30. King, N., Westbrook, M. J., Young, S. L., Kuo, A., Abedin, M., Chapman, J., Fairclough, S., Hellsten, U., Isogai, Y., Letunic, I., Marr, M., Pincus, D., Putnam, N., Rokas, A., Wright, K. J., Zuzow, R., Dirks, W., Good, M., Goodstein, D., Lemons, D., Li, W., Lyons, J. B., Morris, A., Nichols, S., Richter, D. J., Salamov, A., Sequencing, J. G., Bork, P., Lim, W. A., Manning, G., Miller, W. T., McGinnis, W., Shapiro, H., Tjian, R., Grigoriev, I. V., and Rokhsar, D. (2008) The genome of the choanoflagellate *Monosiga brevicollis* and the origin of metazoans. *Nature* **451,** 783–788
31. Lang, B. F., O'Kelly, C., Nerad, T., Gray, M. W., and Burger, G. (2002) The closest unicellular relatives of animals. *Curr. Biol.* **12,** 1773–1778
32. Vicente-Manzanares, M., Ma, X., Adelstein, R. S., and Horwitz, A. R. (2009) Non-muscle myosin II takes centre stage in cell adhesion and migration. *Nat. Rev. Mol. Cell Biol.* **10,** 778–790
33. Ikebe, M., Koretz, J., and Hartshorne, D. J. (1988) Effects of phosphorylation of light chain residues threonine 18 and serine 19 on the properties and conformation of smooth muscle myosin. *J. Biol. Chem.* **263,** 6432–6437
34. Kamisoyama, H., Araki, Y., and Ikebe, M. (1994) Mutagenesis of the phosphorylation site (serine 19) of smooth muscle myosin regulatory light chain and its effects on the properties of myosin. *Biochemistry* **33,** 840–847
35. Bresnick, A. R., Wolff-Long, V. L., Baumann, O., and Pollard, T. D. (1995) Phosphorylation on threonine 18 of the regulatory light chain dissociates

the ATPase and motor properties of smooth muscle myosin II. *Biochemistry* **34,** 12576–12583
36. Umemoto, S., Bengur, A. R., and Sellers, J. R. (1989) Effect of multiple phosphorylations of smooth muscle and cytoplasmic myosins on movement in an *in vitro* motility assay. *J. Biol. Chem.* **264,** 1431–1436
37. Colburn, J. C., Michnoff, C. H., Hsu, L. C., Slaughter, C. A., Kamm, K. E., and Stull, J. T. (1988) Sites phosphorylated in myosin light chain in contracting smooth muscle. *J. Biol. Chem.* **263,** 19166–19173
38. Miller-Hance, W. C., Miller, J. R., Wells, J. N., Stull, J. T., and Kamm, K. E. (1988) Biochemical events associated with activation of smooth muscle contraction. *J. Biol. Chem.* **263,** 13979–13982
39. Seto, M., Sasaki, Y., and Sasaki, Y. (1990) Stimulus-specific patterns of myosin light chain phosphorylation in smooth muscle of rabbit thoracic artery. *Pflügers Arch.* **415,** 484–489
40. Seto, M., Sasaki, Y., Hidaka, H., and Sasaki, Y. (1991) Effects of HA1077. A protein kinase inhibitor, on myosin phosphorylation and tension in smooth muscle. *Eur. J. Pharmacol.* **195,** 267–272
41. Takeya, K., Loutzenhiser, K., Wang, X., Kathol, I., Walsh, M. P., and Loutzenhiser, R. (2011) Differing effects of angiotensin II on myosin light chain phosphorylation in renal afferent and efferent arterioles. *FASEB J.* **25,** 817a
42. Seto, M., Yano, K., Sasaki, Y., and Azuma, H. (1993) Intimal hyperplasia enhances myosin phosphorylation in rabbit carotid artery. *Exp. Mol. Pathol.* **58,** 1–13
43. Harada, T., Seto, M., Sasaki, Y., London, S., Luo, Z., and Mayberg, M. (1995) The time course of myosin light-chain phosphorylation in blood-induced vasospasm. *Neurosurgery* **36,** 1178–1182
44. Katsumata, N., Shimokawa, H., Seto, M., Kozai, T., Yamawaki, T., Kuwata, K., Egashira, K., Ikegaki, I., Asano, T., Sasaki, Y., and Takeshita, A. (1997) Enhanced myosin light chain phosphorylations as a central mechanism for coronary artery spasm in a swine model with interleukin-1β. *Circulation* **96,** 4357–4363
45. Shimokawa, H., Seto, M., Katsumata, N., Amano, M., Kozai, T., Yamawaki, T., Kuwata, K., Kandabashi, T., Egashira, K., Ikegaki, I., Asano, T., Kaibuchi, K., and Takeshita, A. (1999) Rho kinase-mediated pathway induces enhanced myosin light chain phosphorylations in a swine model of coronary artery spasm. *Cardiovasc. Res.* **43,** 1029–1039
46. Obara, K., Nishizawa, S., Koide, M., Nozawa, K., Mitate, A., Ishikawa, T., and Nakayama, K. (2005) Interactive role of protein kinase C-δ with Rho kinase in the development of cerebral vasospasm in a canine two-hemorrhage model. *J. Vasc. Res.* **42,** 67–76
47. Walsh, M. P., Valentine, K. A., Ngai, P. K., Carruthers, C. A., and Hollenberg, M. D. (1984) Ca^{2+}-dependent hydrophobic-interaction chromatography. Isolation of a novel Ca^{2+}-binding protein and protein kinase C from bovine brain. *Biochem. J.* **224,** 117–127
48. Ngai, P. K., Carruthers, C. A., and Walsh, M. P. (1984) Isolation of the native form of chicken gizzard myosin light-chain kinase. *Biochem. J.* **218,** 863–870
49. Takeya, K., Loutzenhiser, K., Shiraishi, M., Loutzenhiser, R., and Walsh, M. P. (2008) A highly sensitive technique to measure myosin regulatory light chain phosphorylation. The first quantification in renal arterioles. *Am. J. Physiol. Renal Physiol.* **294,** F1487–1492
50. Sherry, J. M., Górecka, A., Aksoy, M. O., Dabrowska, R., and Hartshorne, D. J. (1978) Roles of calcium and phosphorylation in the regulation of the activity of gizzard myosin. *Biochemistry* **17,** 4411–4418
51. Gratecos, D., and Fischer, E. H. (1974) Adenosine 5′-*O*-(3-thiotriphosphate) in the control of phosphorylase activity. *Biochem. Biophys. Res. Commun.* **58,** 960–967
52. Cassidy, P., Hoar, P. E., and Kerrick, W. G. (1979) Irreversible thiophosphorylation and activation of tension in functionally skinned rabbit ileum strips by [^{35}S]ATPγS. *J. Biol. Chem.* **254,** 11148–11153
53. Walsh, M. P., Bridenbaugh, R., Kerrick, W. G., and Hartshorne, D. J. (1983) Gizzard Ca^{2+}-independent myosin light chain kinase. Evidence in favor of the phosphorylation theory. *Fed. Proc.* **42,** 45–50
54. Bialojan, C., Rüegg, J. C., and Takai, A. (1988) Effects of okadaic acid on isometric tension and myosin phosphorylation of chemically skinned guinea pig taenia coli. *J. Physiol.* **398,** 81–95
55. Craig, M., Luu, H. A., McCready, T. L., Williams, D., Andersen, R. J., and Holmes, C. F. (1996) Molecular mechanisms underlying the interaction of motuporin and microcystins with type-1 and type-2A protein phosphatases. *Biochem. Cell Biol.* **74,** 569–578
56. Grassie, M. E., Moffat, L. D., Walsh, M. P., and MacDonald, J. A. (2011) The myosin phosphatase targeting protein (MYPT) family. A regulated mechanism for achieving substrate specificity of the catalytic subunit of protein phosphatase type 1δ. *Arch. Biochem. Biophys.* **510,** 147–159
57. Cho, Y. E., Ahn, D. S., Morgan, K. G., and Lee, Y. H. (2011) Enhanced contractility and myosin phosphorylation induced by Ca^{2+}-independent MLCK activity in hypertensive rats. *Cardiovasc. Res.* **91,** 162–170
58. Somlyo, A. P., and Somlyo, A. V. (2003) Ca^{2+} sensitivity of smooth muscle and nonmuscle myosin II. Modulated by G proteins, kinases, and myosin phosphatase. *Physiol. Rev.* **83,** 1325–1358